Published in Journal of Biological Chemistry 284, issue 5, 2603-2616, 2009
which should be used for any reference to this work

Characterization of Tic110, a Channel-forming Protein at the Inner Envelope Membrane of Chloroplasts, Unveils a Response to Ca^{2+} and a Stromal Regulatory Disulfide Bridge*

Mónica Balsera[‡§1], Tom A. Goetze[¶], Erika Kovács-Bogdán[‡§], Peter Schürmann[‖], Richard Wagner[¶], Bob B. Buchanan[§], Jürgen Soll[‡§], and Bettina Bölter[‡§]**

*From the [‡]Munich Center for Integrated Protein Science CiPS[M], Ludwig-Maximilians-Universität München, Feodor-Lynen-Strasse 25, D-81377 Munich, Germany, the [§]Department Biologie I-Botanik, Ludwig-Maximilians-Universität, Grosshadernerstrasse 2-4, D-82152 Planegg-Martinsried, Germany, the [¶]Department of Biophysics, University of Osnabrück, Barbarastrasse 13 D-49076 Osnabrück, Germany, the [‖]Laboratorie de Biologie Moléculaire et Cellulaire, Université de Neuchâtel, Rue Emile-Argand 11, CH-2009 Neuchâtel, Switzerland, and the **Department of Plant and Microbial Biology, University of California, Berkeley, California 94720*

Tic110 has been proposed to be a channel-forming protein at the inner envelope of chloroplasts whose function is essential for the import of proteins synthesized in the cytosol. Sequence features and topology determination experiments presently summarized suggest that Tic110 consists of six transmembrane helices. Its topology has been mapped by limited proteolysis experiments in combination with mass spectrometric determinations and cysteine modification analysis. Two hydrophobic transmembrane helices located in the N terminus serve as a signal for the localization of the protein to the membrane as shown previously. The other amphipathic transmembrane helices are located in the region composed of residues 92–959 in the pea sequence. This results in two regions in the intermembrane space localized to form supercomplexes with the TOC machinery and to receive the transit peptide of preproteins. A large region also resides in the stroma for interaction with proteins such as molecular chaperones. In addition to characterizing the topology of Tic110, we show that Ca^{2+} has a dramatic effect on channel activity *in vitro* and that the protein has a redox-active disulfide with the potential to interact with stromal thioredoxin.

After the proposed endosymbiotic event that gave rise to chloroplasts and, as a consequence, to the massive transfer of genes from the endosymbiont to the host cell nucleus, two new machineries were developed at the outer and inner envelope of chloroplasts, the TOC and TIC complexes, respectively. The machineries transport plastid proteins, whose synthesis was moved to the cytosol, back to the plastid (for a review, see Refs. 1 and 2). Whereas the channel of the TOC complex is homologous to the Omp85 family of transporters in bacteria (3), the TIC complex shows no homology to known transport systems, since the plasma membrane-bacterial transport machineries were relocated to the thylakoid membrane. Moreover, there was an essential requirement for establishing new lines of communication between the organelle and other parts of the cell (4). In chloroplasts of land plants, redox regulation is linked to oxygen and/or light. The regulation of chloroplast-specific processes by redox in accord with the status of the organelle applies not only for transcription and translation but also for translocation. Redox regulation at the translocation level has been proposed for the TIC machinery on the basis of protein composition and dynamics (5–8) as well as specific *in vitro* import experiments (9). However, despite advances in our biochemical understanding of the import process, little is presently known regarding details of the role of redox or of the structure of the TIC complex, particularly with respect to its channel subunits.

Tic110 is essential for protein import into plastids (10–12). It has been proposed to be a pore-forming protein and one of the main components of the TIC complex (13). Previous studies have provided information about certain aspects of Tic110 structure-function. The region from residue 93 to 602 (*Arabidopsis* sequence) is involved in the formation of joint translocation sites between the TOC and the TIC complex (12). Part of the region (residues 185–370 in *Arabidopsis* sequence) contains a binding site for the transit peptide (14). In addition, Tic110 coordinates the chaperone complex system in the stroma in order to complete the translocation process. The protein forms a ternary complex with Tic40 and Hsp93, and at least certain of the Tic110 residues (331–553 and 602–966, *Arabidopsis* sequence) are implicated in the binding (12). The interaction with Tic32, a proposed redox- and Ca^{2+}-regulated member of the TIC machinery, was localized to the N-terminal region of Tic110 (residues 39–231 in pea) (7).

Electrophysiological characterization of a truncated version of Tic110 that lacks the two hydrophobic transmembrane helices at the N terminus (Tic110ΔN) in reconstituted planar lipid

* This work was supported by Deutsche Forschungsgemeinschaft Grant SFB594, Fundación Ramón Areces (to M. B.), International Max-Planck Research School for Life Sciences (to E. K. B.), and Bayerische Hochschulzentrum für Mittel-, Ost-, und Südosteuropa (to E. K. B.). The costs of publication of this article were defrayed in part by the payment of page charges. This article must therefore be hereby marked "*advertisement*" in accordance with 18 U.S.C. Section 1734 solely to indicate this fact.

[1] To whom correspondence should be addressed: Dept. of Structural Biology, Paul Scherrer Institut, CH-5232 Villigen PSI, Switzerland. Tel.: 41-563104047; Fax: 41-563105288; E-mail: monica.balsera@psi.ch.

bilayers revealed properties of a cation-selective channel, sensitive to chloroplast transit peptides (13). Two different models have been proposed to explain the topology of Tic110. The models agree on the arrangement of the two hydrophobic transmembrane helices located at the N terminus, which have been shown to contain essential information on localizing the protein to the inner envelope membrane (15), but they disagree on Tic110ΔN protein organization. Whereas one model considers that it resides in the chloroplast stroma, the other proposes that certain loops lie in the intermembrane space. The first model was developed from evidence obtained with a truncated C-terminal protein expressed in soluble form in *Escherichia coli* (14) and limited proteolysis studies carried out with isolated chloroplast and inner envelope membrane preparations (16). The same experiments performed by our group, however, led to different conclusions (13, 15). The electrochemical properties of Tic110 in lipid bilayers firmly support the second model.

In view of present discrepancies, a more systematic analysis of the topology of Tic110 is clearly timely. Herein, we provide evidence that supports the electrophysiological features of Tic110 as a channel and, in addition, show that Ca^{2+} has a dramatic effect on Tic110 channel activity. Experimental and computational methods have been combined to map the topology of the protein at the inner envelope membrane of pea chloroplasts and to obtain useful structural insight. Based on these analyses, we propose a model in which Tic110ΔN has four amphipathic transmembrane segments. This would lead to two large regions located in the intermembrane space of chloroplasts and a large component in the stroma. The model reconciles the experimental results published so far on Tic110. Interestingly, six conserved Cys in the Tic110 sequence of vascular plants are positioned in the stromal compartment where they have the potential to undergo regulation via thioredoxin (Trx).[2]

EXPERIMENTAL PROCEDURES

Bacteria and Plasmids—Pisum sativum Tic110 (psTic110, residues 1–959) cloning and transformation were previously described (15). The coding region of the C-terminal region of the Tic110 protein from pea (psTic110ΔN, residues 96–959) was amplified by PCR (15) and cloned into pET21d. The plasmids were transformed into BL21(DE3) *E. coli* cells.

Protein Purification—psTic110 was overexpressed in *E. coli* as inclusion bodies. The protein was purified in-batch by Ni^{2+}-nitrilotriacetic acid (Amersham Biosciences) in 20 mM Tris-HCl, 500 mM NaCl, 250 mM imidazol, 8 M urea, pH 7.9. The purified protein was refolded by dilution in 50 mM Tris-HCl, 250 mM NaCl, 1 mM EDTA, 0.03% *n*-dodecyl-β-D-maltoside (DDM), pH 7.9, concentrated, and run over a size exclusion column (Superdex 200; Amersham). In the case of psTic110ΔN, the soluble fraction after cell disruption was applied to a His-Trap HP column (Amersham Biosciences), which was equilibrated with 20 mM Tris-HCl, 300 mM NaCl, pH 7.9. The protein was eluted with 100 mM imidazol and applied to a Superdex 200 column. Size exclusion chromatography (Superose 6; Amersham) coupled to static light scattering (SLS) was used in complementation to 6.5–12% Blue Native-polyacrylamide gels to test the oligomerization state of the psTic110ΔN protein.

Isolation of Inner Envelope Vesicles—Membrane fractions enriched in right side-out inner envelope vesicles (IEV) of chloroplast membranes were isolated from intact chloroplasts from 10–12-day-old pea plants as described previously (17). The native Tic110 band was excised after SDS-PAGE, and protein was eluted from gel pieces in the presence of 80 mM nonanoyl-*N*-methylglucamide before reconstitution into liposomes.

Proteoliposome Preparation and Flotation Assay—Lipid vesicles (PC, fraction IV, azolectin; Sigma) were prepared as previously reported (18) in buffer containing 10 mM Mops/Tris, 100 mM NaCl, pH 7.0, 1% SDS. Liposome-associated and liposome-free proteins were separated by flotation through a sucrose gradient. The proteoliposome and the liposome-free protein sample were adjusted to a sucrose concentration of 1.6 M (2 ml) and overlaid with 9 ml of a step sucrose gradient (0.8, 0.4, 0.2, and 0.1 M). The samples were centrifuged at 100,000 × *g* for 19 h at 4 °C. 1-ml fractions were collected and precipitated with trichloroacetic acid. The samples were resuspended in Laemmli buffer and analyzed by SDS-PAGE (10% gel) and stained with silver.

Electrophysiological Measurements—Small unilamellar liposomes were obtained from purified phosphatidylcholine (from egg, Larodan Fine Chemicals AB) by dissolving 20 mg/ml in 100 mM NaCl, 10 mM Mops/Tris, pH 7, and then sonicating in a water bath for 30 s (300H Omnilab Laborzentrum GmbH & Co. KG). Nonanoyl-*N*-methylglucamide was added up to a final concentration of 80 mM prior to the addition of an equal volume of protein-containing eluate (concentrated to approximately 1 mg of protein/ml). The mixture was incubated for 1.5 h at room temperature and subsequently dialyzed against 100 mM NaCl, 10 mM Mops/Tris, pH 7, for 22 h. The planar lipid bilayer measurements were performed as described previously (19). For a compilation of a representative current-voltage relationship of gating events, the difference of the respective current levels (open and more closed state) was taken from nine independent bilayers (approximately 1380 gating events). These data were classified and averaged based on a statistical presentation in a histogram.

Limited Proteolysis Assays in IEV—Ten μg of IEV were resuspended in 10 μl of buffer (50 mM Tricine-KOH, pH 8.5, 0.1 mM $CaCl_2$) and treated with 0.001, 0.01, and 0.1 μg/μl trypsin (Sigma) for 90 s at 20 °C. The reaction was stopped by adding excess soybean trypsin inhibitor (Roche Applied Science) and macroglobulin (Roche Applied Science). The membranes were pelleted and washed in 10 mM Tricine-KOH, pH 8.5, in the presence of both trypsin inhibitors. Proteolysis experiments were also performed with thermolysin (Calbiochem) and endoproteinase Glu-C (Roche Applied Science). In the proteolysis experiments with thermolysin, IEV were resuspended in 10 μl of 25 mM Hepes-KOH, pH 7.6, 5 mM $MgCl_2$, 0.5 mM $CaCl_2$ and

[2] The abbreviations used are: Trx, thioredoxin; AMS, 4-acetamido-4′-maleimidylstilbene-2,2′-disulfonic acid; DDM, *n*-dodecyl-β-D-maltoside; IEV, inner envelope vesicles; IMS, intermembrane space; MS, mass spectrometry; TCEP, Tris(2-carboxyethyl)phosphine; PEG-MAL, metoxypolyethylenglycol-maleimide; SEC, size exclusion chromatography; Mops, 4-morpholinepropanesulfonic acid; Tricine, *N*-[2-hydroxy-1,1-bis(hydroxymethyl) ethyl]glycine; DTT, dithiothreitol; pS, picosiemens; BisTris, 2-[bis-(2-hydroxyethyl)amino]-2-(hydroxymethyl)propane-1,3-diol.

treated with 0.001, 0.01, and 0.1 μg/μl thermolysin at 20 °C. After 2 min, the reaction was stopped by the addition of 10 mM EDTA. In a parallel experiment, IEV were resuspended in 10 μl of 50 mM NH_4HCO_3, pH 7.9, buffer and incubated with 0.01, 0.1, 1, and 4 μg of endoproteinase Glu-C at 20 °C. After 10 min, excess macroglobulin was added. The pelleted membranes were washed in buffer in the presence of macroglobulin. The recovered membranes were then solubilized in Laemmli buffer with 4 M urea and subjected to SDS-PAGE (8–14%) and immunoblotting using polyclonal antibody against Tic110.

Peptide Fingerprint Mapping by Mass Spectrometry (MS)—The processed bands of Tic110 after trypsin digestion were sliced from SDS-PAGE and subjected to in-gel trypsin digestion. The protein extracted from the gel was analyzed by a combination of matrix-assisted laser desorption ionization time-of-flight and liquid chromatography/MS/MS analyses in the Protein Analysis Unit at the Adolf-Butenandt-Institute (Ludwig-Maximilians-Universität, Munich, Germany). To exclude degradation by endogenous proteases during sample preparation, the samples without trypsin were also analyzed by MS. The rough localization of cleavage sites for some of the proteolytic fragments after trypsin digestion of IEV proceeded as follows. First, the MASCOT program (20) (mass tolerance = 20; missed cleavage sites = 0 or 1) was used to analyze the mass spectrometry data and identify fragments in the Tic110 sequence from pea. Then a region of Tic110 was assigned to each fragment, and the molecular weight of the fragment was compared with the molecular mass obtained in the SDS-PAGE. Considering the secondary structure prediction and assuming that the proteolysis reaction would preferentially occur in residues that do not belong to secondary structure elements (21), a likely cleavage site is proposed. For some of the fragments, the N-terminal or C-terminal amino acid was detected, thus allowing a more precise estimation.

Pegylation Assays—IEV were treated with 10 mM metoxypolyethylenglycol-maleimide (5,000 Da) (PEG-MAL; Laysan) in a buffer containing 0.1 M Tris-HCl, pH 7.0, 1 mM EDTA, for 0, 5, 10, and 20 min, at 4 °C in the dark. The pegylation reaction was stopped by adding Laemmli buffer in the presence of 100 mM DTT. NuPAGE BisTris gels (7.5%) were employed using a Mops running buffer. The protein was detected by immunoblotting.

CD Spectroscopy—The secondary structure of psTic110ΔN was analyzed by far-UV CD spectroscopy. The protein was dialyzed against 20 mM potassium phosphate, pH 8.0, and the protein concentration was adjusted to 3 μM. The CD spectrum was measured at 10 °C using a J-780 spectropolarimeter with a 1-mm optical path length cell over a wavelength range from 185 to 260 nm. The CD spectrum represents the average of four accumulations at a scanning speed of 20 nm/min and 1 nm spectral bandwidth. Protein concentration was estimated by the extinction coefficient at 280 nm in 6 M guanidine hydrochloride under reducing conditions, using the molar absorption coefficient calculated from the ExPASy server (available on the World Wide Web). The quantification of the secondary structure elements was estimated with the SELCON3 (22), CDSSTR (23), CONTIN/LL (24), and CDNN (25) programs.

Analysis of Tic110 Structure by Computational Methods—A Blast search (26) was performed, using psTic110 as input, to retrieve all known sequences belonging to the Tic110 family. The multiple sequence alignment of the Tic110 family was performed by TCoffee (27) and visually inspected. Internal repetition motifs, disorder regions, and hydropathy plots were predicted from the sequences by the MEME (28), PONDR (29), and MPEx (30) programs, respectively. The PROF (31), PSIPRED (32), PORTER (33), and SSpro 4.0 (34) programs were used to predict the secondary structure. The 3DPSSM (35), FUGUE (36), 123D+ (37), and PHYRE (38) threading programs were employed in an attempt to assign a fold to Tic110.

Influence of Oxidizing/Reducing Conditions in Tic110—psTic110ΔN was incubated with 50 μM $CuCl_2$ or 10 mM DTT at 20 °C. After 1 h, the protein was trichloroacetic acid-precipitated (5% final concentration), and the pellet was washed with acetone and dissolved in a freshly prepared buffer containing 10 mM 4-acetamido-4′-maleimidylstilbene-2,2′-disulfonic acid (AMS; Invitrogen), 2 mM EDTA, 0.1 M Tris-HCl, pH 7.0. Proteins were separated by nonreducing SDS-PAGE (8.5%) and Coomassie-stained. To check the reversibility of the redox reaction, a stock of psTic110ΔN (2 μM, soluble or reconstituted into liposomes) was oxidized with 50 μM $CuCl_2$, dialyzed to remove the oxidant, and incubated with several concentrations of DTT (0.05–10 mM) or Trx (1 μM) from *E. coli* (Sigma) in the presence of either DTT (0.05, 0.5 mM) or NADPH Trx reductase (0.5 μM)/NADPH (2.5 mM). The capability of stromal *f* and *m* Trxs (1 μM) to reduce Tic110 was assayed in the presence of 0.5 mM DTT.

Redox State of Tic110 in Darkness—The redox state of native Tic110 was analyzed in freshly prepared chloroplasts isolated in the dark. Chloroplasts were either untreated or treated with 50 μM $CuCl_2$ or 2 mM Tris(2-carboxyethyl)phosphine (TCEP; Sigma) at 20 °C. After 30 min of incubation and solubilization (1% SDS), 10 mM AMS was added. The solubilized chloroplasts were subjected to SDS-PAGE (8.5%), and Tic110 was visualized by immunodecoration.

RESULTS

Purification of Recombinant psTic110ΔN from Pea—psTic110ΔN (residues 96–959 from pea sequence; Fig. 1*A*), which lacks the two predicted transmembrane helices at the N terminus, was cloned into pET21d vector. The affinity purification of psTic110ΔN with a His-Trap column consistently resulted in three species of apparent molecular mass of about 100, 60, and 20 kDa (Fig. 1*B*, *lane a*). Immunoblotting with monoclonal anti-His tag antibodies showed that each of the three proteins contained the tag (data not shown). Edman degradation was therefore carried out to determine the N-terminal sequence of each protein. The first fragment obviously corresponded to the first residues of the psTic110ΔN plasmid; the second and the third obtained the N-terminal sequences, MADSKA and MKQIR, respectively, which correspond to internal fragments of the Tic110 protein. A closer look at the DNA sequence revealed the presence of two likely ribosome binding sites (RBS) (GGGGAG and GGGAAG) near a methionine residue (Met^{433} and Met^{788}, respectively; Fig. 1*A*). Each binding site may turn into a "new" Tic110 translation initiation

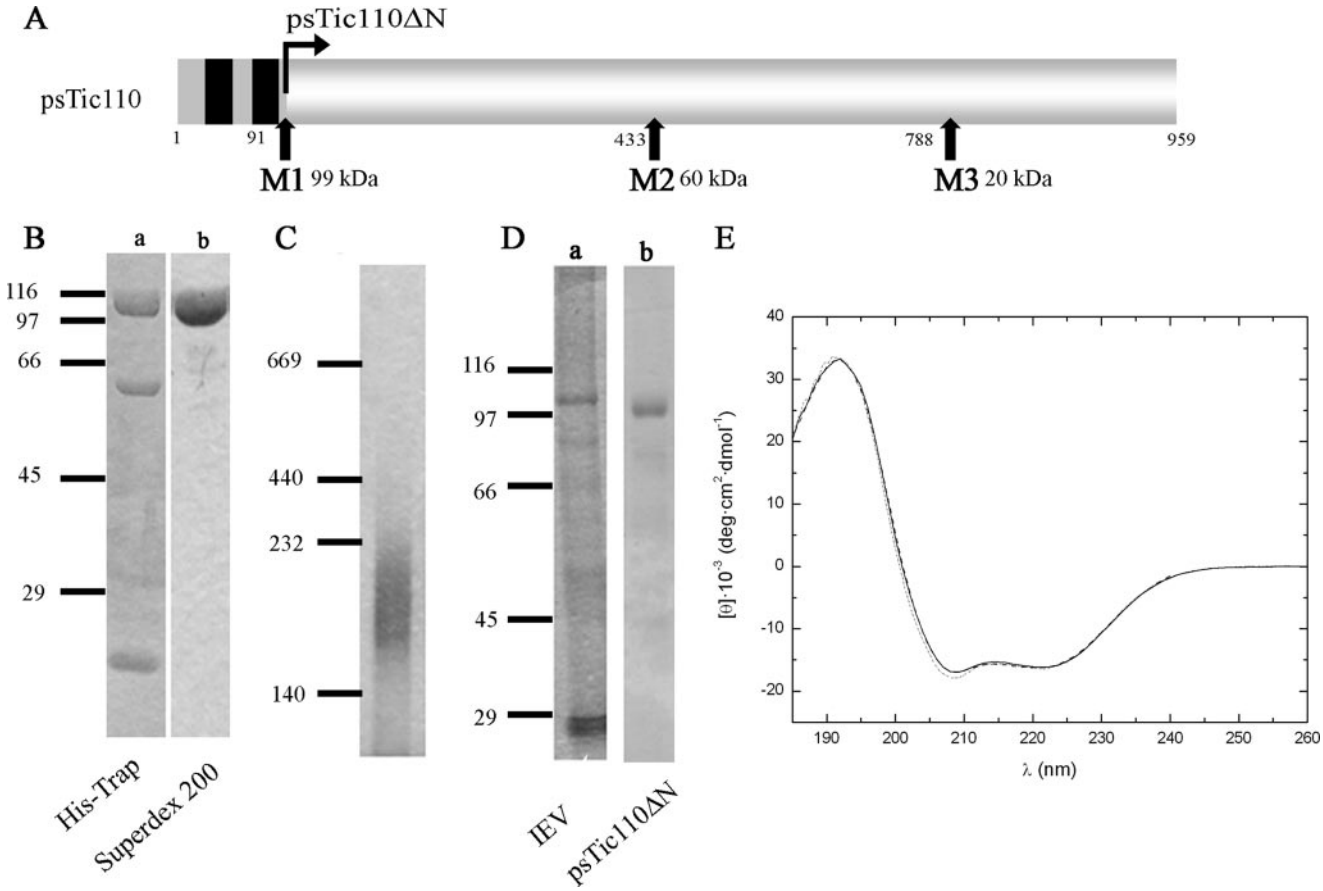

FIGURE 1. **Purification and characterization of recombinant Tic110 from pea.** *A*, Tic110 sequence is made up of two regions, an N-terminal region (residues 1–91) that contains two putative transmembrane helices and a C-terminal hydrophilic region (residues 92–959); *B*, psTic110ΔN and psTic110 were purified to homogeneity. After the purification with a His-Trap column, three bands are recognized in SDS-PAGE and by anti-His tag antibody. N-terminal sequencing indicates that psTic110ΔN contains three alternative initial translation sites when overexpressed in *E. coli*, designated psTic110ΔN or M1 (residues 91–959), M2 (residues 433–959), and M3 (residues 788–959), as pointed out in the sequence in *A*; *C*, Blue Native-polyacrylamide gel electrophoresis shows that psTic110ΔN is a dimer, in agreement with SEC-SLS experiments (data not shown); *D*, nonreducing SDS-PAGE of IEV and psTic110ΔN indicates that covalent bonds are not involved in dimerization; *E*, secondary structure of psTic110ΔN by far-UV CD. The analysis of the far-UV CD spectrum of Tic110 indicates that it is composed of about 53% α-helix, 8% β-strand, and 38% nonregular elements of secondary structure. The *continuous* and *short dash dot* lines represent psTic110ΔN in the absence and presence of detergent (0.03% DDM), respectively; the *dashed line* shows the fitted curve in the absence of detergent.

sites when overexpressed in *E. coli*. These two fragments are designated M2-psTic110ΔN (60 kDa) and M3-psTic110ΔN (20 kDa), respectively. The three proteins, including psTic110ΔN (99 kDa), could be adequately separated by size exclusion chromatography (SEC) (Fig. 1*B*, *lane b*). For some experiments, we took advantage of the second and third truncated forms of Tic110 from pea. The full-length protein (psTic110) was purified from inclusion bodies by His tag affinity column and refolded by dilution. The protein was further purified by SEC (Fig. 2*B*).

psTic110ΔN Behaves as a Dimer in Solution—Blue Native-polyacrylamide gel electrophoresis (Fig. 1*C*) and SEC-SLS (data not shown) clearly show that psTic110ΔN is actually a dimer (195 kDa), although the retention volume of psTic110ΔN in SEC corresponds to a globular protein of 400 kDa (Fig. 2*A*). The dimer is in equilibrium with minor amounts of tetramer. These differences are probably due to the fact that Tic110 is an elongated, nonglobular dimer, with a Stokes radius similar to that of a 400-kDa globular protein. Reinjection of the purified psTic110ΔN dimer onto the size exclusion column gave a single peak at the same elution volume, thus indicating that the dimer is stable at concentrations between 0.1 and 1.5 mg/ml. Higher concentrations were not yet tested. Attempts to create monomeric species of psTic110ΔN, changing conditions such as ionic strength (0–1 M NaCl), adding detergents (0.01–1% DDM) or pH (6.5–8), failed, suggesting that monomer formation is unstable in solution. SEC in combination with nonreducing SDS-PAGE showed that intermolecular disulfide bridges are not implicated in dimer formation. Thus, neither the retention volume nor the peak area changed in the presence of 10 mM DTT, and dimers were not visible in nonreducing SDS-PAGE in either the IEV or psTic110ΔN preparation (Fig. 1*D*, *lanes a* and *b*, respectively). Nevertheless, SDS-PAGE revealed monomer bands, confirming their presence under denaturing conditions.

psTic110ΔN Binds Detergents and Liposomes—The capability of psTic110ΔN to bind detergents and phospholipid vesicles was assessed, respectively, by SEC and flotation experiments. Interestingly, SEC revealed that, unlike M3-psTic110ΔN, the retention volumes for psTic110ΔN and M2-psTic110ΔN downshifted significantly in the presence of detergent (0.03–1% DDM) (Fig. 2*A*). The shift in retention volume of psTic110ΔN and M2-psTic110ΔN approximate the running behavior of the full-length Tic110 (Tic110), indicating that they share similar hydrodynamic properties and, therefore, a similar conforma-

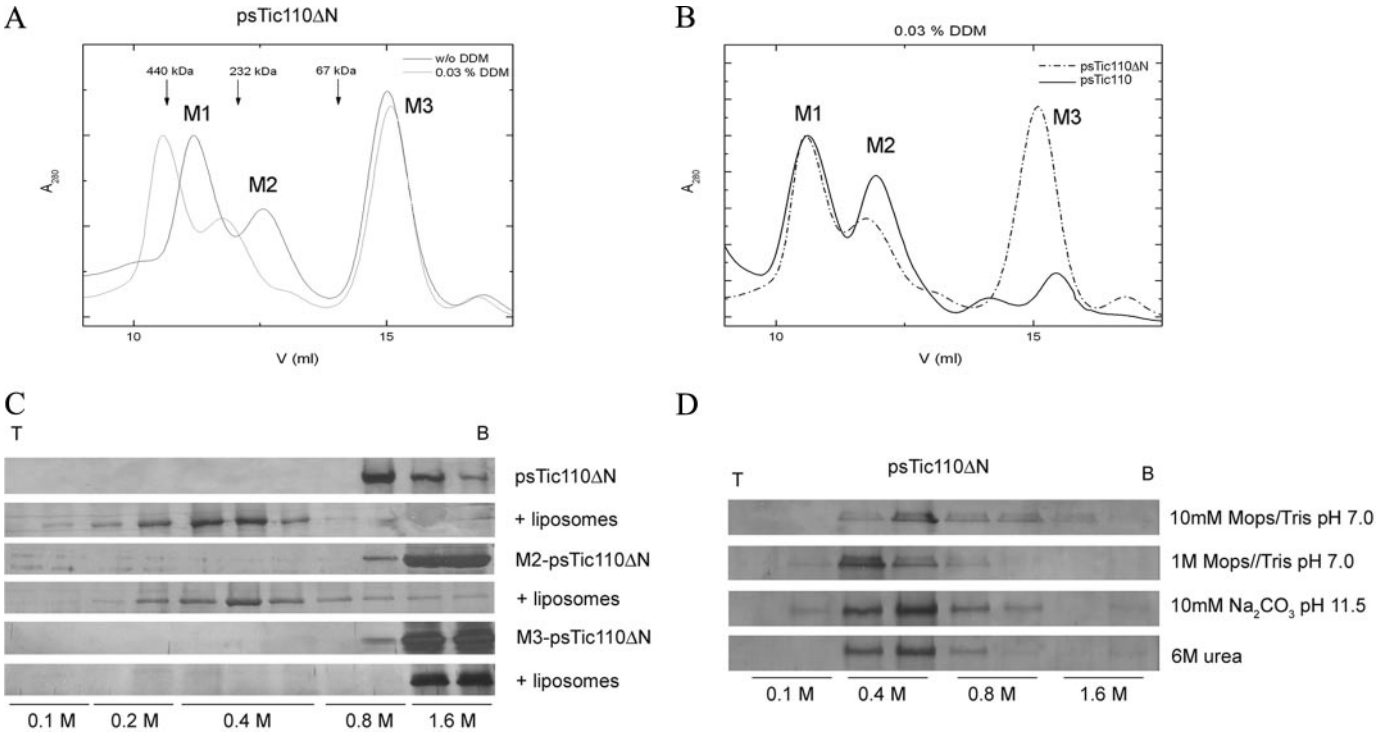

FIGURE 2. **Tic110 association with detergents and incorporation into liposomes.** *A*, Superdex 200 SEC profile of psTic110ΔN in the absence or presence of detergent (0.03% DDM). The three peaks correspond to the three truncated versions of psTic110ΔN, namely M1, M2, and M3. The profile was assayed both in the presence and absence of detergent. A shift in the elution volume of M1 and M2, toward higher molecular weight species in the presence of detergent suggests that both M1 and M2 bind detergent molecules. Reload of M1 and M2 alone in the size exclusion column does not change the elution volume, indicating that the dimer is stable in solution. The *arrows* indicate the retention volumes of soluble mass standard proteins; *B*, comparison of the SEC profiles of psTic110ΔN and psTic110 in the presence of 0.03% DDM. In the presence of detergent, both proteins show similar hydrodynamic properties, suggesting a similar overall conformation. *C*, flotation experiments of psTic110ΔN and M2- and M3-psTic110ΔN in liposome-free form or in proteoliposomes. Purified psTic110ΔN was incubated with liposomes, and its insertion was assayed by flotation analyses in a discontinuous sucrose gradient (1.6-0.1 M sucrose). Liposome-free psTic110ΔN and M2- psTic110ΔN protein is recovered at the bottom of the gradient (1.6 M), whereas the protein after incubation with liposomes floats at 0.4 M sucrose. However, M3-psTic110ΔN is not incorporated into the liposomes and remains at the bottom even after the incubation with liposomes; *D*, washing of psTic110ΔN proteoliposomes. After their preparation, psTic110ΔN proteoliposomes were washed with an increase in ionic strength (1 M Mops/Tris, pH 7.0), pH 11 (10 mM sodium carbonate), and urea (6 M), and the proteoliposomes were subjected to a flotation assay. In all cases, psTic110ΔN floats at 0.4 M sucrose, indicating that the incorporation of the protein is not due to nonspecific aggregation on the surface of the lipids. *T*, top; *B*, bottom. The sucrose concentration of each analyzed sample is indicated at the *bottom* of the figure.

tion (Fig. 2*B*). Given that the presence of DDM did not affect the retention volume of the soluble proteins ferritin (440 kDa) and catalase (232 kDa) (data not shown), the lower retention volumes for psTic110ΔN and M2-psTic110ΔN suggest an association of the Tic110 proteins with the detergent. In another experiment, the isolated protein was incubated with liposomes in an attempt to produce functional proteoliposomes of psTic110ΔN, as previously reported (13). The insertion of the protein into the liposomes was assayed by flotation in a sucrose concentration gradient. In the absence of liposomes, psTic110ΔN stayed at the bottom of the sucrose gradient, whereas in the presence of phospholipids, the protein floated to the middle of the gradient (Fig. 2*C*). This result shows that psTic110ΔN reduces its density by binding to liposomes. The same experiment was also performed with the truncated versions of psTic110ΔN from pea (see above). M2-psTic110ΔN was able to bind to liposomes, like psTic110ΔN, whereas M3-psTic110ΔN, which stayed at the bottom of the gradient both in the presence or absence of liposomes, has no capability to bind to liposomes (Fig. 2*C*). To confirm that the interaction of psTic110ΔN with the liposomes did not involve nonspecific aggregation on the lipid surface, the proteoliposomes were washed with 6 M urea, 0.01 M sodium carbonate (pH 11), or higher ionic strength (1 M Mops/Tris, pH 7.0) for 30 min at 20 °C. Subsequently, the treated liposomes were subjected to flotation (Fig. 2*D*). The results demonstrate that psTic110ΔN is not simply attached but is inserted in the liposomes. These effects with detergent and liposomes, detected both on psTic110ΔN and M2-psTic110ΔN but not on M3-psTic110ΔN, suggest that Tic110 contains regions sensitive to detergents and lipids between residues 91 and 788 (pea sequence).

psTic110ΔN Is Mainly an α-Helical Protein in Solution and in the Presence of Detergents—The secondary structure of psTic110ΔN was analyzed by far-UV CD in solution in both the absence and presence of detergent (0.03– 0.05% DDM) (Fig. 1*E*). The high α-helical content dominates the spectrum of the psTic110ΔN protein with characteristic minima of ellipticity at 220 and 208 nm and maxima at 193 nm. The average and S.D. calculated for the results obtained with the four different programs yielded the following values: 53 $\pm$ 2% for α-helix, 8.4 $\pm$ 0.5% for β-strand, and 38 $\pm$ 3% for turn/nonregular structure. Only slight differences are detectable in the presence of detergents, suggesting that the main elements of the secondary structure are maintained under these conditions.

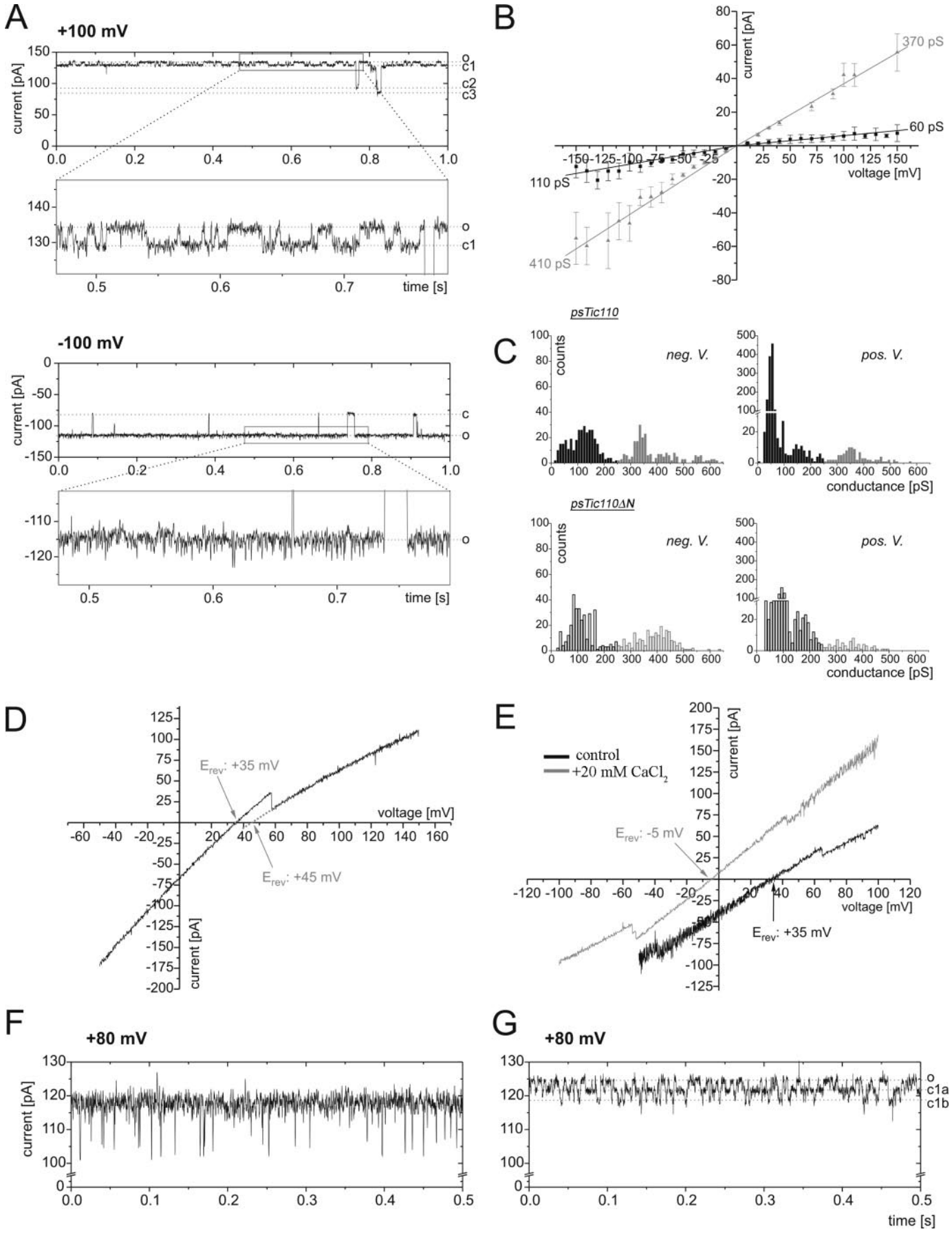
A
+100 mV
current [pA]
o
c1
c2
c3
time [s]
-100 mV
c
o
B
current [pA]
370 pS
60 pS
110 pS
410 pS
voltage [mV]
C
psTic110
counts
neg. V.
pos. V.
conductance [pS]
psTic110ΔN
D
E_rev: +35 mV
E_rev: +45 mV
voltage [mV]
E
control
+20 mM CaCl2
E_rev: -5 mV
E_rev: +35 mV
F
+80 mV
G
+80 mV
c1a
c1b

In Vitro Gating Behavior and Conductance of Tic110 in Lipid Bilayers—After fusion of proteoliposomes containing native psTic110 or psTic110ΔN with planar lipid bilayers, ion channel activity could be observed (Fig. 3, *A*, *F*, and *G*). The total channel conductance of a single fusion process was quite large and rather variable, with an average on the order of 2 nanosiemens ($n_{\text{independent bilayers}} = 17$, S.D. of ± 1.2 nanosiemens) under symmetrical electrolyte conditions (250 mM KCl). After single fusion events, integration of further proteoliposomes could be prevented by electrolyte perfusion directly after the first fusion. The observed amplitudes of individual single gating events were comparatively heterogeneous, ranging from single channel amplitudes between $\Lambda_{\text{small}} \cong 50$ pS to $\Lambda_{\text{large}} \cong 600$ pS (Fig. 3*C*). The analysis of the connectivity of the single channel gating events (Fig. S1*A*) indicates that the different gating amplitudes can be attributed to a single active channel unit, as previously observed for other protein translocation channels (39, 40). Moreover, the presence of a large pore with multiple conductance states and high flexibility was suggested by several observations. First, gating events of both small and large conductance states were observed simultaneously in all experiments (Fig. 3, *B* and *C*). If this behavior were due to two independent channels, every single proteoliposome fused with the planar membrane would have to contain both pore-forming proteins in the active form. This appears very unlikely, especially since a potential second fusion with another liposome was prevented by perfusion. These conductance properties were observed with both native psTic110 and psTic110ΔN proteoliposomes.

A fingerprint in Tic110 channel activity was a rapid gating event with a conductance of 60–110 pS in 250 mM KCl (Fig. 3, *A–C*, *squares* and *bars*). These gating transitions exceeded all other observed gating events with respect to the frequency of occurrence (see Fig. 3*C*) and showed a characteristic voltage dependence (*i.e.* the channel was much more active at either positive or negative holding potentials). Because this feature is side-specific, the gating characteristic can be used to determine the channel's orientation within the bilayer that turned out to be randomly distributed. To compile comparable conductance histograms (Fig. 3*C*) data of individual experiments were corrected for their relative orientation within the bilayer. Gating events were classified into two classes based on the histograms (threshold value 250 pS). Events of higher conductance (>250 pS) were quite heterogeneous and distributed over a rather wide range. However, from the distribution of the gating events, we can conclude that in most experiments only one or two active channels were incorporated into the bilayer. The number of fusion processes supports this conclusion as well as the corresponding number of levels of the small (60–110 pS) gating amplitude. The conductance of the completely open Tic110 channel can therefore be estimated to be on the order of $\Lambda \cong 600$ pS (in 250 mM KCl; Fig. 3*C*).

In summary, the observed channel characteristics of the native psTic110 and psTic110ΔN channels were similar to each other (Fig. 3, *A* and *C*; supplemental Fig. S1*B*) and were also comparable with the overall conductance of other protein translocation channels, namely Tim22 and Sec61 (39, 40).

Ion Selectivity—The selectivity of Tic110 was measured under asymmetric salt conditions (*cis*/*trans* 250/20 mM KCl and/or vice versa). In general, both native and psTic110ΔN channels exhibited cationic selectivity. Interestingly, the degree of selectivity, as determined from the reversal potential (V_{rev}), was dependent on the open state of the pore (Fig. 3*D*). Most frequently, V_{rev} values of $V_{\text{rev}} = +35$ mV and $V_{\text{rev}} = +45$ mV were observed. Using the constant field Goldman-Hodgkin-Katz approach (41), these values correspond to a selectivity of $P_{K^+}/P_{Cl^-} = 6{:}1$ and 11:1, respectively. Interestingly, as seen below, an inversion of selectivity in the presence of Ca^{2+} was observed.

Ca^{2+} Ions Influence Tic110 Channel Properties—Under asymmetric conditions, the addition of $CaCl_2$ resulted in a dramatic change in the reversal potential (Fig. 3*E*, from $V_{\text{rev}} = +35$ mV to $V_{\text{rev}} = -5$ mV), corresponding to an inversion of selectivity. This effect cannot be attributed to changes in ionic composition but rather to drastic changes in the charge distribution on the surface of the channel pore. Moreover, the presence of Ca^{2+} in the buffer solution exerted a strong effect on channel gating. Directly after fusion of a proteoliposome with the planar lipid bilayer, the channel showed the characteristic activity described above, consisting of resolved, rapid (60–110 pS) gating (Fig. 3*A*). However, after perfusion of the chambers to symmetric conditions and removal of Ca^{2+}, a rather unstructured flickering current was observed in most of the cases (Fig. 3*F*). This flickering, unstable state of the channel could be converted back to a well defined slower gating state by the addition of $CaCl_2$ (20 mM; see Fig. 3*G*). The effect seems to be specifically ascribable to Ca^{2+}, since Mg^{2+} or a decrease of the overall ionic strength showed no comparable effect (data not shown).

FIGURE 3. **Electrophysiological properties of native psTic110 and psTic110ΔN.** *A*, current traces of a bilayer containing one or two active native Tic110 channels at holding potentials of $V_m = +100$ mV (*top*) and -100 mV (*bottom*). For clarity, a *zoom* into the *trace* is shown in *boxes*. The *dotted lines* indicate the current levels of the open (*o*) and several more closed states of the channel (*c1–c3*). A characteristic rapid gating between the open and the closed state "c1" is obvious at positive voltages. At negative voltages, these small current transitions are missing or at least less frequent, whereas larger gating events still appear. Electrolytes in *A*, *B*, *C*, and *F* were symmetrical (250 mM KCl, buffered with 10 mM Mops/Tris, pH 7); *B* and *C*, current-voltage relationship and conductance histogram taken, respectively, from the differential current amplitude of all analyzed gating events. Data were classified and averaged with reference to *C*. A small and rapid gating (60 and 110 pS, respectively) is characteristic for the native (*filled symbols* and *bars*) and the psTic110ΔN channel (*open bars*). Larger gating events (370 and 410 pS) occur but are relatively variable in amplitude. Both proteins display a similar distribution of gating events. The number of independent bilayers is as follows: native Tic110, $n = 9$ (1,378 events); psTic110ΔN, $n = 3$ (552 events). *D*, the native Tic110 channel is cation-selective under asymmetric buffer conditions (*cis*/*trans* 250/20 mM KCl). The current signal of a voltage ramp between -50 and $+150$ mV is shown. The reversal potential of an open state of the channel is $+35$ mV, whereas the extrapolated value of a more closed state is $+45$ mV; *E*, the selectivity of the Tic110 channel (native and psTic110ΔN) is influenced by Ca^{2+} ions. After the addition of 20 mM $CaCl_2$ to both electrolytes, the reversal potential shifts from $+35$ mV (control, *darker*) to -5 mV. Conditions were as in *D*. *F*, current trace of two native Tic110 channels under symmetric electrolyte conditions (250 mM KCl) at a holding potential of $+80$ mV. The channels are in a state of hyperactive flickering. Broadened noise amplitude supersedes the initially ordered, small, and rapid gating. Larger gating events may take place but happen below time resolution; *G*, current trace of the same bilayer as in *F* after the addition of 20 mM of $CaCl_2$ (*cis* and *trans*) and stirring for 2 min. Gating behavior is reverted to an ordered and rapid manner within time resolution. The *dotted lines* denote an open and two more closed current levels (*c1a*, *b*). These gating events resemble the same transitions as in *A* (*top*), *o* to *c1*.

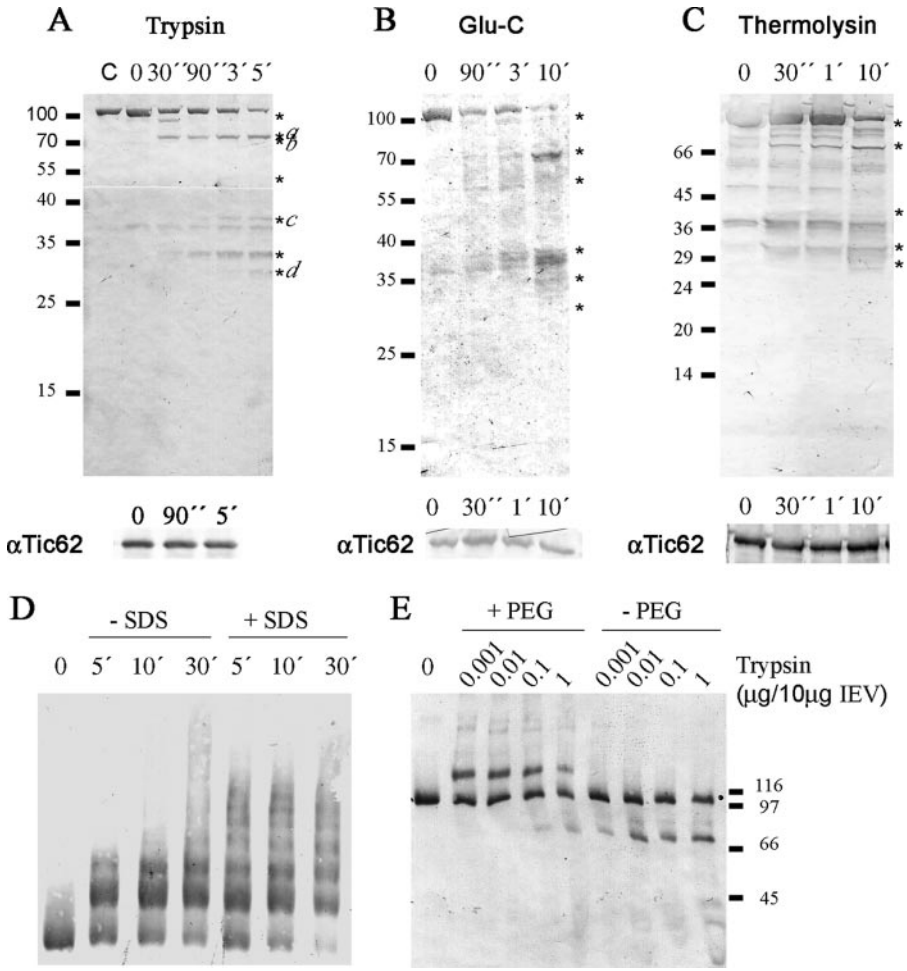

FIGURE 4. **Proteolytic fragmentation and pegylation assays of Tic110 in IEV.** Incubation of IEV with trypsin (0.1 μg/10 μg of IEV) (*A*), endoproteinase Glu-C (4 μg/10 of μg IEV) (*B*), and thermolysin (0.1 μg/10 μg of IEV) (*C*) for different times. The *asterisks* point to the proteolytic fragments of Tic110 detected by immunodecoration. The similarity in the digestion pattern from the three different proteases suggests a specific proteolytic reaction within Tic110 regions orientated toward the IMS. The *control lane* in *A* demonstrates the effectiveness of the quenching reaction, in which the quenching mixture was added to the protein sample preceding the incubation with the protease. At the *bottom*, the digestion of Tic62 under the same conditions is shown. The insensitivity of Tic62 to proteases demonstrates that the proteases do not cross the membrane under these conditions and also that IEV have a right side-out orientation. The sequences of the proteolytic fragments *a–d* after trypsin digestion were obtained by MS (Table 1). *D*, after incubation with PEG-MAL (5,000 Da), IEV were run on a 7.5% acrylamide BisTris gel and immunodecorated using antibodies against Tic110. Intact IEV (*−SDS*) or solubilized IEV (+1% SDS (*+SDS*)) were incubated with PEG-MAL for 5, 10, and 30 min. One prominent higher molecular weight band, which corresponds to one modified Cys, is visible after 5 min of reaction, whereas more than seven modified Cys residues are marked in solubilized membranes under the same conditions. *E*, trypsin digestion of modified IEV with PEG-MAL (*PEG*). Different concentrations of trypsin (1, 0.1, 0.01, and 0.001 μg/10 μg of IEV) were incubated with IEV for 90 s, pretreated or not with PEG-MAL. It demonstrates that pegylation affects digestion of Tic110 in IEV by trypsin and that the 77-kDa fragment band is not modified with PEG-MAL.

Native Tic110 in IEV Is Sensitive to Proteases That Cannot Cross the Envelope Membrane under Controlled Conditions—The proteolytic sensitivity of Tic110 in isolated inner envelope vesicles was assayed with three different proteases that were previously reported not to cross the inner envelope membrane of chloroplasts under controlled conditions: trypsin and endoproteinase Glu-C, whose activity is extinguished with an excess of serine inhibitors (such as soybean trypsin inhibitor, phenylmethylsulfonyl fluoride, and macroglobulin), and thermolysin, which can be easily quenched with EDTA (Fig. 4, *A–C*). Tic62 is proposed to attach to the inner envelope membrane at the stromal face, not exposed to the IMS (8, 42), and is, therefore, useful as control for the proteolysis experiments presented here. To control the quenching reaction of the protease adequately, one sample was initially incubated with the proteinase inhibitor mixture prior to adding the protease. Fig. 4, *A–C*, shows immunodecorations of Tic110 and Tic62 in IE after treatment with trypsin, endoproteinase Glu-C, and thermolysin. It is concluded that Tic110 is sensitive to proteases, whereas Tic62 remains intact after protease treatment under the same conditions. In addition, it is demonstrated that trypsin can be properly quenched with an excess of soybean trypsin inhibitor and macroglobulin (Fig. 4*A*, *control lane*), and no residual activity is present after solubilization of the membranes. The control reaction with Tic62 shows the correct orientation of the inner envelope vesicles. These experiments corroborate earlier results showing that parts of Tic110 are present in the chloroplast intermembrane space (15).

Identification of Tic110 Proteolytic Peptides—Immunoblot analysis using an antibody raised against Tic110 (Fig. 4) showed that short incubation times gave rise to two proteolytic fragments of ~95 and ~77 kDa. Whereas the 95-kDa fragment was quickly processed, the 77-kDa counterpart was quite stable under the conditions used. This fragment was unequivocally identified by MS to correspond to residues 311–959 (Table 1 and Fig. 4, fragment *a*). Other fragments (73, 54, 38, 34, and 30 kDa) appear with increasing incubation time (Fig. 4) or increasing protease concentration (data not shown). Fragments of 73, 38, and 30 kDa were also identified by MS (Table 1). Comparable proteolytic fragments were obtained when using thermolysin and endoproteinase Glu-C instead of trypsin (Fig. 4), illustrating that proteolytic fragmentation occurs in unique regions in Tic110.

The four fragments identified by MS, portions of Tic110 that are retained in the membrane after the proteolysis reaction, were mapped onto the Tic110 sequence, as described under "Experimental Procedures." Possible cleavage sites are proposed based on a combination of molecular mass estimation and secondary structure predictions, giving priority to residues that are located in loop regions and are not inserted in stable secondary structure elements. Fragment *a* (Table 1 and Fig. 4*A*) has been identified as containing the C-terminal amino acid

TABLE 1
Proteolytic fragments of Tic110 identified by MS after trypsin digestion of IEV

Fragment	Mass (SDS)	Mass (MS)	Residue range (MS)	Percentage of coverage	Number of matching peptides	Cleavage sites (mass of proposed fragment)
	kDa	*kDa*		*%*		
a	77	73	311–959	41	22	Arg^{276} (76.6 kDa)
b	73	70	1–655	25	11	Arg^{663} (72.5 kDa)
c	38	31.2	658–942	15	3[a]	Arg^{618} (38.5 kDa)
d	30	30	1–287	28	5[a]	Arg^{287} (30 kDa)

[a] Missed cleavage sites = 0.

phenylalanine (Phe^{959}, pea sequence). Considering the MS results, the first residue of this fragment would be Arg^{310}, which results in a fragment of 73 kDa, slightly less than the one estimated by SDS-PAGE (77 kDa). The cleavage site could therefore be 30–50 residues upstream of position 311. The compatible arginine/lysine residues could be Lys^{264}, Lys^{269}, and Arg^{276}. On the basis of the molecular mass estimated by SDS-PAGE, the likely cleavage point is Arg^{276}. Similar reasoning was employed to localize the cleavage site of the other three fragments. The results are summarized in Table 1. These experiments demonstrate that regions of Tic110 comprising residues Arg^{276}, Arg^{663}, Arg^{618}, and Arg^{287} are located in the IMS of chloroplasts.

Cys Mapping by Pegylation—To confirm further that regions of Tic110 are situated in the IMS, we carried out pegylation experiments in IEV using PEG-MAL (5,000 Da) as a probe. PEG-MAL is a membrane-impermeable probe that reacts irreversibly with sulfhydryl groups of Cys, adding 5 kDa for each SH blocked. After pegylation, the number of higher mass bands in SDS-PAGE should correspond to the number of Cys that reacted with PEG-MAL. Thus, this is an ideal method to localize Cys residues in regions of Tic110 oriented toward the IMS. Accordingly, IEV were treated with PEG-MAL, and the reaction was followed by SDS-PAGE and immunoblotting (Fig. 4*D*). One very prominent band of higher molecular mass was recognized after incubation with PEG-MAL. A second band was also visible and became more prominent after longer incubation times, perhaps due to different accessibility toward PEG-MAL. Under the same conditions in the presence of detergent, when PEG-MAL could react with stromal Cys, the Tic110 antibody recognized a ladder of seven or more bands of higher molecular mass. In an attempt to relate the above proteolytic experiments with the results obtained with PEG-MAL, limited trypsin digestion of IEV was performed after pegylation. The aim was to determine whether both reactions take place at equivalent positions (*i.e.* in specific regions of Tic110 confined to the IMS). If so, sensitivity to trypsin should be affected by pegylation. The proteolytic experiments showed that trypsin had less access to Tic110 in IEV previously incubated with PEG-MAL (Fig. 4*E*), indicating that the proteolytic sites in Tic110 are more protected following derivatization. The 77-kDa proteolytic fragment did not change its mass under these conditions, demonstrating that the modified Cys is located elsewhere, perhaps between residues 1 and 275. Two Cys are present in this region in pea Tic110, namely Cys^{134} and Cys^{275}. It is concluded that one of these Cys is located in the IMS region of Tic110.

Secondary Structure and Fold Recognition by Computational Methods—Because no high or low resolution structure is available for Tic110, we undertook the design of a topological model of the membrane-localized protein by combining computational methods with experimental data. Tic110 is present in all chloroplast-containing organisms (43). A multiple sequence alignment of the Tic110 family is presented as supplemental material (Fig. S2). Secondary structure predictions estimate that Tic110 is mainly an α-helix protein (57% α-helix, 3% β-strand, and 40% turn/nonregular structure) (Fig. 5*A*). This is in agreement with data from far-UV CD measurements (Fig. 1*E*). Except for a short helix predicted in land plants but not green algae (H^{338}SDIDRLARG; pea sequence), no large differences were found in the protein among photosynthetic eukaryotes (sequence identity > 30%). Large differences were found, however, between green plants (land plants and green algae) and nongreen algae. Two very long insertions characterize the non-green algae members (data not shown), one at the end of the second hydrophobic transmembrane helix of the N terminus and another in a region predicted to face the IMS (see below). All sequences (green plants and non-green algae) contain the two N-terminal hydrophobic helices predicted to be transmembrane and a less conserved but highly negatively charged region (residues 598–627 in pea sequence; Fig. 5*A*) predicted to be disordered by the PONDR program (29). Six fully conserved Cys in vascular plants (Cys^{134}, Cys^{445}, Cys^{492}, Cys^{506}, Cys^{674}, and Cys^{890} in the pea sequence) are potential candidates for metal coordination or participation in a disulfide bridge. Sequence analysis of green plant Tic110 by the MEME algorithm (28), which searches for motifs in groups of related proteins, identified six repetitions predicted to contain a helix-loop-helix element of secondary structure (Fig. 5*A*, *underlined*). These repetitions are also found in the non-green algal sequences although at a higher number (data not shown).

Examination of the pea Tic110 sequence by the MPEx program (30), based on the Wimley-White scale of hydrophobicity, revealed that the partition free energy for the region of residues 208–226 makes an association with the nonpolar region unfavorable. Residues 666–684 and 697–715 are two other regions with similar but even lower probability. In addition, an in depth analysis of predicted helices by helical plots shows that some have amphipathic features (numbers according to the mature pea sequence): helix A (L^{208}IYVSNIVFGDASSFLLPW); helix B (A^{311}VPGVSQVVEELEKVLSFNDLLI); helix C (T^{546}ALSIASKAVRRMFITYV); helix D (K^{577}ELKKLIAFNTLVVTKLVEDI); and helix E (A^{664}DLYKTFLTYCLTGDVV) (Fig. 5*A*). Helices A and E are among those suggested by the MPEx program, and they represent promising candidates for being inserted into the membrane.

Because proteins similar to Tic110 were not found in structure-related databases, we performed fold recognition by *threading*. Threading servers retrieved several fold templates

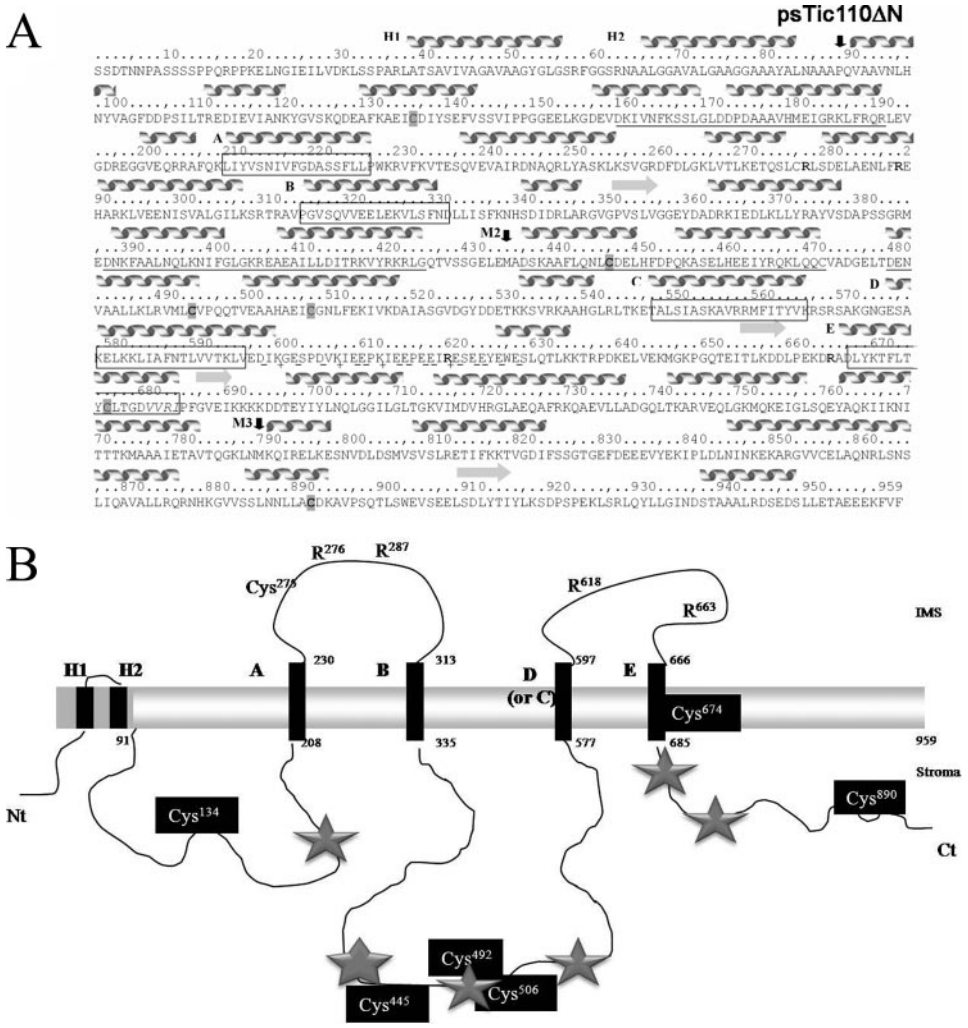

FIGURE 5. *A*, sequence features of Tic110 from pea *P. sativum* Tic110 mature protein sequence and secondary structure prediction. The secondary structure prediction is annotated *above* the sequence. *Spirals* and *arrows* represent α-helical and β-strand elements of secondary structure, respectively. The beginning of psTic110ΔN and the truncated versions M2- and M3-psTic110ΔN are indicated with *perpendicular arrows*. The two putative hydrophobic transmembrane helices at the N terminus are named as H1 and H2. The four putative amphipathic transmembrane regions in psTic110ΔN are shown in *boxes* (*A–E*). The end of helix E (in *italics*) is weakly predicted to be an α-helix. The helix-loop-helix repetition motifs are *underlined*. The cleavage sites obtained by MS after trypsin digestion of IEV (Fig. 4) are shown in *boldface type*. The charge of the amino acids of the less conserved and disorder-predicted region between residues 600 and 625 is annotated *below* the sequence. Six conserved Cys in vascular plants (Cys^{134}, Cys^{445}, Cys^{492}, Cys^{506}, Cys^{674}, and Cys^{890}) are *shaded*. *B*, proposed topological model for Tic110 in the membrane. Tic110 pea sequence has been used as guide. Two hydrophobic helices (H1 and H2) and four amphipathic helices (*A*, *B*, *C* or *D*, and *E*) form the putative transmembrane region of Tic110 at the inner envelope membrane of chloroplasts. Two regions are therefore placed in the IMS (230–313 and 597–666). The residues Arg^{276}, Arg^{287}, Arg^{618}, and Arg^{663} were obtained as cleavage sites after limited trypsin digestion of IEV (Fig. 4). Pegylation experiments show that one Cys of Tic110 is in the IMS (Fig. 4). In our model, Cys^{275} would be located in the IMS and would perfectly match the results obtained in the proteolytic digestion of IEV after pegylation (Fig. 5). A second Cys, Cys^{674}, is situated in the pore-lining region and may be susceptible to derivatization by PEG-MAL after longer incubation times. The *stars* represent the six helix-loop-helix repetition motifs found by MEME (28) in green plant Tic110 sequences. In parallel with the HEAT motif repetitions in other proteins, it is speculated here that they cluster together, creating a proper environment for receiving the preprotein.

that, interestingly, were related to proteins consisting of helical unit repetitions. Those templates with ARM/HEAT repeats were statistically significant as defined by the authors of the threading programs (more than 80% certainty), and their secondary structures largely matched that predicted for Tic110. The Protein Data Bank codes of the hit templates included 1b3u (pr65α protein), 1qgr (importin-β), and 1u6g (Cand1 protein) as well as 1avc (annexin VI) and 1cii (colicin I). All are α proteins that consist of conformational helix motif repetitions. It is known that HEAT repeats occur either in tandem arrays (between 3 and 22 repetitions) or are dispersed throughout the sequence. Although degenerate in sequence (composed of 37–43 residues), they contain a consensus pattern of conserved hydrophobic residues (44). The secondary structural elements of the HEAT repeats fit well with the repetition motifs found in Tic110. Moreover, they suggest that Tic110 contains more than six repetitions (as earlier noted for non-green algae) that seem to be degenerated and therefore difficult to detect by direct sequence comparison.

Topological Model of Tic110—From the above and previously reported results, it can be concluded that: (*a*) parts of the region composed of residues 91–778 (pea sequence) interact with lipids (this work); (*b*) regions that contain residues Arg^{276}, Arg^{287}, Arg^{618}, and Arg^{663} (pea sequence) are located in the IMS (this work); (*c*) parts of the region composed of residues 331–553 and 602–966 (*Arabidopsis* sequence) are located in the stroma to interact with the Hsp93-Tic40 complex (12); (*d*) parts of the region composed of residues 93–602 (*Arabidopsis* sequence) are located in the IMS to be able to contact the TOC complex (12); (*e*) part of the region composed of residues 39–231 (pea sequence) is located in the stroma to interact with Tic32 (7); and (*f*) helix unit repetitions in an antiparallel helix fashion cluster together similar to the HEAT motif arrangement (this work). The two first transmembrane helices were described as being essential for targeting Tic110 to the chloroplast inner envelope. Because M2-psTic110ΔN (but not M3-psTic110ΔN) is able to bind to liposomes, a second, lipid-inserted portion of Tic110 is concluded to be located between residues 93 and 658, where the amphipathic helices are found. The combination of these observations with secondary structure analysis and arrangement of amphipathic helices provides an explanation for the limited proteolysis experiments with inner envelope vesicles (*i.e.* that the regions of residues 230–313 and 570–666 (pea sequence) are oriented toward the

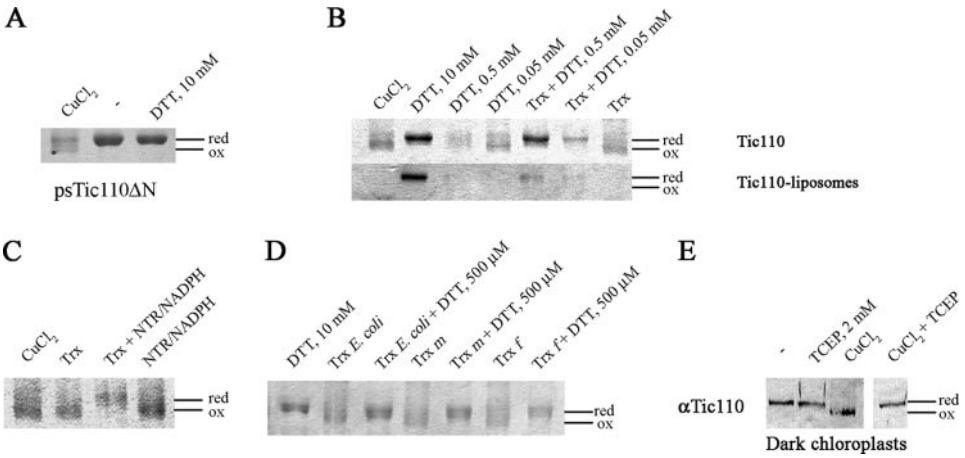

FIGURE 6. **Redox state of Tic110.** *A*, psTic110ΔN is isolated in a reduced state. The oxidized (*ox*) and reduced (*red*) forms generated after $CuCl_2$ (50 μM) and DTT (10 mM) incubation, respectively, are shown for comparison; *B*, oxidized psTic110ΔN (after $CuCl_2$ treatment) was reversibly reduced with 10 mM DTT or 1 μM Trx (*E. coli*) plus 0.05/0.5 mM DTT, but not with 0.05 or 0.5 mM DTT alone, both in soluble form and after reconstitution in liposomes, indicating the presence of a putative regulatory disulfide bridge in both states; *C*, oxidized psTic110ΔN is reduced by *E. coli* Trx previously reduced with NADPH Trx reductase (*NTR*) (*E. coli*) and NADPH, its physiological reductant, instead of DTT; *D*, oxidized psTic110ΔN can be also reduced with 1 μM Trxs *f* and *m* (two specific stromal Trxs) in the presence of 0.5 mM DTT, suggesting a physiological role for Trx regulating Tic110 activity; *E*, redox state of Tic110 in chloroplasts in the dark. The protein is reduced under these conditions but is oxidized with 50 μM $CuCl_2$ and reversibly reduced with 2 mM TCEP ($CuCl_2$ + TCEP).

IMS). Therefore, there are six transmembrane helices in our topological working model for Tic110 (see "Discussion"), with at least two large regions in the IMS and a bulk part in the stroma (Fig. 5*B*).

psTic110ΔN Shows Different Redox States in Vitro—Multiple sequence alignment of Tic110 family members shows six conserved Cys residues in vascular plants. This observation prompted us to determine the *in vitro* redox state of Tic110. To this end, we alkylated free sulfhydryl groups with AMS after incubating the protein under oxidizing ($CuCl_2$) or reducing (DTT) conditions. The presence of an intramolecular disulfide bridge was detectable by a decrease in mobility of the reduced form compared with the oxidized counterpart in nonreducing SDS-PAGE (AMS added 500 Da to the molecular mass per reactive thiol). Our results show that psTic110ΔN was recovered in reduced form after purification (Fig. 6*A*, *lane 2*). As previously observed with other proteins (45), oxidized Tic110 ran as a diffuse band that was less stainable with Coomassie than the reduced form. Furthermore, the appearance of different bands in nonreducing SDS-PAGE after incomplete oxidation with $CuCl_2$ suggests that Tic110 was present in different redox states. The kinetic and thermodynamic properties of the oxidized and reduced forms of Tic110 are interesting subjects of future investigation.

To assess the reversibility between the oxidized and reduced states, a stock solution of Tic110 was oxidized by $CuCl_2$ and, after dialysis, was incubated with 0.05, 0.5, and 10 mM DTT (Fig. 6*B*). The recovery of the reduced form with 10 mM DTT is evidence for the presence of at least one redox-active disulfide bridge.

To determine whether the disulfide bridge responds to a physiological reductant, oxidized Tic110 was incubated with Trx (*E. coli*), itself reduced with an amount of DTT (0.5 mM) insufficient for reduction by itself (Fig. 6*B*). The results show that psTic110ΔN was effectively reduced by Trx when tested either in soluble form or after reconstitution into liposomes, indicative of a putative regulatory disulfide bridge. Tic110 was also reduced by Trx, itself reduced by NADPH and NADPH Trx reductase rather than DTT (Fig. 6*C*). The reduction of Tic110 was further examined *in vitro* using Trxs *f* and *m*, two members of the Trx family present in chloroplast stroma. As observed with *E. coli* Trx, the reduced (but not oxidized) forms of both chloroplast Trxs effectively reduced Tic110 (Fig. 6*D*). It is concluded that Tic110 is a potential target of Trx in the stroma of chloroplasts.

Native Tic110 Has a Redox-active Disulfide—The redox state of native Tic110 was assessed in chloroplasts isolated from pea plants in the dark. To simulate the oxidized and reduced forms of Tic110, chloroplast samples were separately treated with $CuCl_2$ and TCEP (Fig. 6*E*). The presence of a putative native disulfide bridge is apparent in the difference in running behavior of membrane-bound Tic110 after treating chloroplasts with $CuCl_2$ or TCEP prior to treatment with AMS and solubilization with SDS. The results revealed that Tic110 was present in a reduced state in chloroplasts maintained in the dark (Fig. 6*E*). In an attempt to convert the reduced to the oxidized form and verify the reversibility of the reaction, isolated chloroplasts were treated first with $CuCl_2$ and then with TCEP prior to derivatizing with AMS. As seen in Fig. 6*E*, the oxidation of Tic110 was reversed with TCEP, confirming the presence of a reversible disulfide bridge in the native protein.

DISCUSSION

The present results demonstrating a functional relation of psTic110ΔN within the inner envelope membrane of chloroplasts provide the basis for a topological model of Tic110. The model places part of the C-terminal region of Tic110 in the IMS and at the same time reconciles experimental results so far published on the protein. This positioning is based on the following observations: (*a*) Tic110 is accessible to proteases that cannot cross the inner envelope of chloroplasts under controlled conditions; (*b*) psTic110ΔN, which lacks the two predicted transmembrane helices, binds to detergents and liposomes; (*c*) psTic110ΔN-proteoliposomes show channel activity *in vitro*; and (*d*) the Tic110 sequence contains helices with amphipathic features.

The present study is the first in which the channel properties of native Tic110 protein have been characterized *in vitro*. The large overall conductance of native Tic110 activity of $\Lambda_{max} \approx$ 600 pS, albeit highly variable in amplitude, indicates that the Tic110 pore is highly flexible but meets the requirements for the transport of substrates, such as partly unfolded preproteins,

with respect to size and selectivity. In principle, the published values of conductance and reversal potential for Tic110 (13) are in line with our recent findings. However, the observed prominent and characteristic rapid gating of about 60–110 pS and high variability in the open channel conductance states have not been reported previously. Other α-helical preprotein translocases (*e.g.* the Sec61p complex of the endoplasmic reticulum or Tim22 and Tim23 complexes of the inner mitochondrial membrane) show comparable values for completely open channels (39, 40, 46). The deduced highly dynamic Tic110 pore, especially, reveals striking similarity to the electrophysiological properties of the Sec61p complex. Except for the rapid 60–110 pS gating, a wide distribution of conductance values with many possible current levels is a unique property of both channels. In addition, an open state-dependent selectivity has also been described for the Sec61p complex,[3] indicative of significant charge displacement in the channel pore during the corresponding conformational transition. The observed channel activity of truncated psTic110ΔN adds an important element to the ongoing discussion on which part of the entire protein constitutes the actual pore. It turns out that the observed electrophysiological properties of psTic110ΔN are very similar to those of native Tic110, thereby confirming the model in which the residues responsible for channel activity are located downstream of amino acid 91 up to the C terminus of the pea chloroplast protein.

The finding that Ca^{2+} acts as an effector of gating and selectivity is quite interesting, since its physiological involvement in the import process is extensively known. It has been shown that Ca^{2+} affects the import of certain substrates at the inner envelope membrane of chloroplast level (47). Further, Tic32, a component of the TIC complex, is described as a calmodulin-binding protein whose reversible association with the TIC machinery is promoted by NADP(H) and Ca^{2+}/calmodulin (5). Thus, by influencing both Tic32 and Tic110, Ca^{2+} would have a double effect on the import machinery. Likely additional factors, such as the presence of other TIC-components, the formation of TOC-TIC supercomplexes, and the interaction with precursor proteins, have a major influence on channel properties *in vivo*.

The presence of transmembrane helices in Tic110ΔN of chloroplasts is also strongly supported by limited proteolysis experiments performed in vesicles enriched in inner envelope membranes of pea chloroplasts. Its sensitivity to proteases that cannot cross the envelope under controlled conditions and the similarity in proteolytic patterns obtained with three different proteases (trypsin, thermolysin, and endoproteinase Glu-C) indicate that patches of psTic110ΔN are positioned in the intermembrane space. The results presently obtained are similar to those of Lübeck *et al.* (15) but clearly contradict those of Jackson *et al.* (16). In the former paper, the authors demonstrated the intactness of the chloroplasts after trypsin treatment by the Hill reaction; in the latter article, it is argued that the sensitivity of Tic110 to trypsin was due to an inadequate quenching of the protease and that digestion took place after lysis of the membranes. Here, we show that the trypsin reaction can be controlled well by adding a protease inhibitor mixture made up of an excess of trypsin inhibitor and macroglobulin. After the addition of trypsin to envelope vesicles that already contained the protease inhibitor mixture, no proteolytic fragments were observed, even after envelope solubilization. Moreover, the proteases did not cross the envelope, as shown by the insensitivity to digestion of Tic62, a TIC complex component proposed to attach to the stromal side of the inner envelope of chloroplasts without crossing the membrane. Although we are aware of the differences between our results and those of Jackson *et al.* (16), we currently have no explanation for their discrepancy.

Two prominent features characterize the model currently proposed: the location of hydrophilic residues in the membrane and the presence of helical repetitions that resemble those of the HEAT motifs. A large number of the HEAT repeats are involved in cytoplasmic transport, where the two helical units appear to function as flexible joints that can wrap around target substrates and act as scaffolding on which other molecular components may assemble (44). The disordered region detected in Tic110 may be important for protein interaction, since the occurrence of negatively charged residues is conserved in all of the sequences of the family. The differences between non-green algae and green plants may be ascribed to a different composition of the TIC complex, given that non-green algae do not contain, for example, the Tic40 or Tic55 components. That truncated versions of the C-terminal region of Tic110 can be expressed in soluble form in *E. coli* was previously shown by Inaba *et al.* (14). It is likely that Tic110 has the ability to bury hydrophobic regions in an aqueous environment so that folding and dimerization come together in solution. The presence of hydrophilic regions in a membrane is not uncommon (48, 49), since buried water molecules or other polar residues may compensate for charges in the membrane; a change in pK_a may also occur in the lipid environment. One of the central questions concerning the topology of the protein-conducting channel of the inner chloroplast envelope is the extent of hydrophilicity of the pore, since the solutes that transport precursor proteins have polar features. Most protein import complexes are formed by hydrophilic channels (*e.g.* SecY/Sec61 (50), Tom40 (51), and Toc75 (52)). The occurrence and importance of amphipathic helices in membrane proteins have been pointed out previously (53).

With respect to topology, the insertion of Tic110 into the membrane and the orientation of its amphipathic helix A toward the IMS (see above) is well supported by previous work (15). These authors demonstrated that a Tic110 construct comprising residues 1–231 in the mature protein (110N-mSSU) was fully located in the membrane of pea chloroplasts and, unlike other constructs (110N1-mSSU, residues 1–111; 110N2-mSSU, residues 112–231), was sensitive to trypsin digestion. These results suggest the presence of an essential region between residues 111 and 231 in Tic110 that crosses the membrane, thereby orienting mSSU to the IMS and rendering it susceptible to protease digestion. The localization of different constructs of Tic110 was also studied in a work with *Arabidopsis* chloroplasts (12). In that case, similar conclusions were

[3] F. Erdmann, personal communication.

made (the constructs atTic110Sol$_{His}$ and atTic110N$_{His}$ are equivalent to the above mentioned constructs 110N2-mSSU and 110N-mSSU, respectively). The results from the construct atTic110C$_{His}$ suggest that residues from 558 to the end in *Arabidopsis* Tic110 sequence also contain information for membrane attachment. The last three regions inserted into the membrane that fit the experimental results are the amphipathic helices B, C/D, and E. Note that in this work we cannot distinguish between helix C or D inserted into the membrane; helix C might be conversely involved in a helix-loop-helix soluble motif (Fig. 5*A*). In the topological model proposed, one Cys of the pea sequence (Cys^{275}) would be exposed to the IMS and therefore susceptible to react with PEG-MAL in inner envelope vesicles, a property that fits with the pegylation results presented. A second Cys (Cys^{674}) might form part of a transmembrane helix channel, whereas the other seven could be located in the stroma. Since the pegylation experiments show a second higher molecular weight band with longer incubation times, this may indicate that one Cys in the pore-lining region is accessible from the outside.

The proposed model of Tic110 explains most of the experimental data published so far and reconciles the two different topological models currently under debate; namely, the C-terminal region is located either in the stroma or intermembrane space. In our opinion, the models are compatible, since a large proportion of the protein is located in the stroma and therefore suitable for interaction with Hsp93 and Tic40 (12) and other components of the TIC machinery. On the other hand, the presence of regions of Tic110 in the intermembrane space would be essential to associate and form supercomplexes with the TOC machinery (12). The interaction of Tic110 with the transit peptide might take place both in the intermembrane space (as with Tim23 (54)) and the stroma during the import process.

The present experiments have uncovered a redox-active disulfide bridge potentially functional in regulating Tic110 via stromal Trx. Although further studies are required, such a disulfide is in accord with the redox regulation of the import process proposed to occur at the inner envelope (55). As discussed above, the conserved Cys residues in Tic110 are restricted to green plants, where the redox regulatory machinery for import was experimentally worked out. Typically, chloroplast proteins that undergo redox regulation by Trx are oxidized in the dark and reduced in the light. The observation that Tic110 is present in the reduced state in chloroplasts in the dark suggests a role in environmental adaptation with Trx as a reductant. It is possible that Trx acts to reactivate Tic110 after an oxidative event. Hence, additional work is needed to determine if Trx affects Tic110 channel activity under normal conditions or if it restores the system following oxidative stress. Recently, Tic55, a regulatory component of the TIC machinery, has been identified as a Trx target (56). It is noteworthy that several Trx-linked chloroplast proteins have been reported to be reduced in the dark (*e.g.* RB60 (57) and 2-Cys Prx (58)). Another Trx target, cyclophilin 20-3 (59), which was in the reduced state when isolated, has been linked to oxidative stress (60). It is conceivable that the activity of the TIC complex is subjected both to metabolic and oxidative regulation.

Acknowledgments—We are very grateful to Dr. L. Lariviere and Prof. P. Cramer for the SEC-SLS experiments and the N-terminal Edman sequencing. We thank P. Benz and A. Stengel for helpful discussions and isolation of dark chloroplasts.

REFERENCES

1. Jarvis, P. (2008) *New Phytol.* **179,** 257–285
2. Stengel, A., Soil, J., and Bolter, B. (2007) *Biol. Chem.* **388,** 765–772
3. Bolter, B., Soll, J., Schulz, A., Hinnah, S., and Wagner, R. (1998) *Proc. Natl. Acad. Sci. U. S. A.* **95,** 15831–15836
4. Pesaresi, P., Schneider, A., Kleine, T., and Leister, D. (2007) *Curr. Opin. Plant Biol.* **10,** 600–606
5. Chigri, F., Hormann, F., Stamp, A., Stammers, D. K., Bolter, B., Soll, J., and Vothknecht, U. C. (2006) *Proc. Natl. Acad. Sci. U. S. A.* **103,** 16051–16056
6. Kuchler, M., Decker, S., Hormann, F., Soll, J., and Heins, L. (2002) *EMBO J.* **21,** 6136–6145
7. Hormann, F., Kuchler, M., Sveshnikov, D., Oppermann, U., Li, Y., and Soll, J. (2004) *J. Biol. Chem.* **279,** 34756–34762
8. Stengel, A., Benz, P., Balsera, M., Soll, J., and Bolter, B. (2008) *J. Biol. Chem.* **283,** 6656–6667
9. Hirohashi, T., Hase, T., and Nakai, M. (2001) *Plant Physiol.* **125,** 2154–2163
10. Schnell, D. J., Kessler, F., and Blobel, G. (1994) *Science* **266,** 1007–1012
11. Wu, C. B., Seibert, F. S., and Ko, K. (1994) *J. Biol. Chem.* **269,** 32264–32271
12. Inaba, T., Alvarez-Huerta, M., Li, M., Bauer, J., Ewers, C., Kessler, F., and Schnell, D. J. (2005) *Plant Cell* **17,** 1482–1496
13. Heins, L., Mehrle, A., Hemmler, R., Wagner, R., Kuchler, M., Hormann, F., Sveshnikov, D., and Soll, J. (2002) *EMBO J.* **21,** 2616–2625
14. Inaba, T., Li, M., Alvarez-Huerta, M., Kessler, F., and Schnell, D. J. (2003) *J. Biol. Chem.* **278,** 38617–38627
15. Lubeck, J., Soll, J., Akita, M., Nielsen, E., and Keegstra, K. (1996) *EMBO J.* **15,** 4230–4238
16. Jackson, D. T., Froehlich, J. E., and Keegstra, K. (1998) *J. Biol. Chem.* **273,** 16583–16588
17. Waegemann, K., and Soll, J. (1995) *Methods Cell Biol.* **50,** 255–267
18. Vojta, A., Scheuring, J., Neumaier, N., Mirus, O., Weinkauf, S., and Schleiff, E. (2005) *Anal. Biochem.* **347,** 24–33
19. Goetze, T. A., Philippar, K., Ilkavets, I., Soll, J., and Wagner, R. (2006) *J. Biol. Chem.* **281,** 17989–17998
20. Perkins, D. N., Pappin, D. J. C., Creasy, D. M., and Cottrell, J. S. (1999) *Electrophoresis* **20,** 3551–3567
21. Fontana, A., de Laureto, P. P., Spolaore, B., Frare, E., Picotti, P., and Zambonin, M. (2004) *Acta Biochim. Pol.* **51,** 299–321
22. Sreerama, N., and Woody, R. W. (2000) *Anal. Biochem.* **287,** 252–260
23. Johnson, W. C. (1999) *Proteins* **35,** 307–312
24. Provencher, S. W., and Glockner, J. (1981) *Biochemistry* **20,** 33–37
25. Dalmas, B., Hunter, G. J., and Bannister, W. H. (1994) *Biochem. Mol. Biol. Int.* **34,** 17–26
26. Altschul, S. F., Madden, T. L., Schaffer, A. A., Zhang, J., Zhang, Z., Miller, W., and Lipman, D. J. (1997) *Nucleic Acids Res.* **25,** 3389–3402
27. Notredame, C., Higgins, D. G., and Heringa, J. (2000) *J. Mol. Biol.* **302,** 205–217
28. Bailey, T. L., Williams, N., Misleh, C., and Li, W. W. (2006) *Nucleic Acids Res.* **34,** W369–W373
29. Dunker, A. K., Lawson, J. D., Brown, C. J., Williams, R. M., Romero, P., Oh, J. S., Oldfield, C. J., Campen, A. M., Ratliff, C. R., Hipps, K. W., Ausio, J., Nissen, M. S., Reeves, R., Kang, C. H., Kissinger, C. R., Bailey, R. W., Griswold, M. D., Chiu, M., Garner, E. C., and Obradovic, Z. (2001) *J. Mol. Graph. Model.* **19,** 26–59
30. Jaysinghe, S., Hristova, K., Wimley, W., Snider, C., and White, S. H. (2006). In
31. Rost, B. (2001) *J. Struct. Biol.* **134,** 204–218
32. Jones, D. T. (1999) *J. Mol. Biol.* **292,** 195–202
33. Pollastri, G., and McLysaght, A. (2005) *Bioinformatics* **21,** 1719–1720
34. Cheng, J., Randall, A. Z., Sweredoski, M. J., and Baldi, P. (2005) *Nucleic Acids Res.* **33,** W72–W76

35. Kelley, L. A., MacCallum, R. M., Sternberg, M. J., Shi, J., Blundell, T. L., and Mizuguchi, K. (2000) *J. Mol. Biol.* **299,** 499–520
36. Shi, J., Blundell, T. L., and Mizuguchi, K. (2001) *J. Mol. Biol.* **310,** 243–257
37. Alexandrov, N. N., Nussinov, R., and Zimmer, R. M. (1996) in *Pacific Symposium on Biocomputing '96* (Hunter, L., and Klein, T. E., eds) pp. 53–72, World Scientific Publishing Co., Singapore
38. Bennett-Lovsey, R., Herbert, A., Sternberg, M., and Kelley, L. (2008) *Proteins* **70,** 611–625
39. Kovermann, P., Truscott, K. N., Guiard, B., Rehling, P., Sepuri, N. B., Muller, H., Jensen, R. E., Wagner, R., and Pfanner, N. (2002) *Mol. Cell* **9,** 363–373
40. Wirth, A., Jung, M., Bies, C., Frien, M., Tyedmers, J., Zimmermann, R., and Wagner, R. (2003) *Mol. Cell* **12,** 261–268
41. Hille, B. (2001) *Ionic Channels of Excitable Membranes*, pp. 445–450, 3rd Ed., Sinauer Associates, Sunderland, MA
42. Balsera, M., Stengel, A., Soll, J., and Bolter, B. (2007) *BMC Evol. Biol.* **7,**
43. McFadden, G. I., and van Dooren, G. G. (2004) *Curr. Biol.* **14,** R514–R516
44. Andrade, M. A., and Bork, P. (1995) *Nat. Genet.* **11,** 115–116
45. Lemker, T., Gruber, G., Schmid, R., and Muller, V. (2003) *FEBS Lett.* **544,** 206–209
46. Meinecke, M., Wagner, R., Kovermann, P., Guiard, B., Mick, D. U., Hutu, D. P., Voos, W., Truscott, K. N., Chacinska, A., Pfanner, N., and Rehling, P. (2006) *Science* **312,** 1523–1526
47. Chigri, F., Soll, J., and Vothknecht, U. C. (2005) *Plant J.* **42,** 821–831
48. Phoenix, D. A., Harris, F., Daman, O. A., and Wallace, J. (2002) *Curr. Protein Pept. Sci.* **3,** 201–221
49. Eyre, T. A., Partridge, L., and Thornton, J. M. (2004) *Protein Eng. Des. Sel.* **17,** 613–624
50. van den Berg, B., Clemons, W. M., Collinson, I., Modis, Y., Hartmann, E., Harrison, S. C., and Rapoport, T. A. (2004) *Nature* **427,** 36–44
51. Hill, K., Model, K., Ryan, M. T., Dietmeier, K., Martin, F., Wagner, R., and Pfanner, N. (1998) *Nature* **395,** 516–521
52. Sveshnikova, N., Grimm, R., Soll, J., and Schleiff, E. (2000) *Biol. Chem.* **381,** 687–693
53. Fernandez-Vidal, M., Jayasinghe, S., Ladokhin, A. S., and White, S. H. (2007) *J. Mol. Biol.* **370,** 459–470
54. Neupert, W., and Herrmann, J. M. (2007) *Annu. Rev. Biochem.* **76,** 723–749
55. Oreb, M., Tews, I., and Schleiff, E. (2008) *Trends Cell Biol.* **18,** 19–27
56. Bartsch, S., Monnet, J., Selbach, K., Quigley, F., Gray, J., von Wettstein, D., Reinbothe, S., and Reinbothe, C. (2008) *Proc. Natl. Acad. Sci. U. S. A.* **105,** 4933–4938
57. Trebitsh, T., Levitan, A., Sofer, A., and Danon, A. (2000) *Mol. Cell Biol.* **20,** 1116–1123
58. Horling, F., König, J., and Dietz, K. J. (2002) *Plant Physiol. Biochem.* **40,** 491–499
59. Motohashi, K., Koyama, F., Nakanishi, Y., Ueoka-Nakanishi, H., and Hisabori, T. (2003) *J. Biol. Chem.* **278,** 31848–31852
60. Dominguez-Solis, J. R., He, Z., Lima, A., Ting, J., Buchanan, B. B., and Luan, S. (2008) *Proc. Natl. Acad. Sci. U. S. A.* **105,** 16386–16391